International Journal of Applied Engineering Research ISSN 0973-4562 Volume 12, Number 21 (2017) pp.11417-11423

FEA of a High Efficiency Brushless DC Motor Design

Manoj Kumar Pandey, Dr. Anurag Tripathi and Dr. Bharti Dwivedi

[1]*Research Scholar, Faculty of Electrical Engineering, Dr. APJ Abdul Kalam Technical University Lucknow, India.*

[2]*Associate Professor, Department of Electrical Engineering, Institute of Engineering and Technology Sitapur Road, Lucknow-226021, India.*

[3]*Professor, Department of Electrical Engineering, Institute of Engineering and Technology Sitapur Road, Lucknow-226021, India.*

Abstract:

This paper describes mathematical modelling and FE analysis of Brushless DC motor. The machine parameter of stator and rotor parts including torque speed characteristics and magnetic analysis are investigate by FE analysis and analytically. The mathematical modelling is carried out by the MATLAB software and FE analysis is carried out by the SPEED software. Parameters of machine is calculated with high accuracy and precision. Seamless investigation can be accomplished by relating the results from above both methods of motor design. The analysis establishes the usefulness of the proposed machines design practice. Permanent Magnet BLDC motor with 1.1 kW rating and 3000 rpm rated speed has been designed and the result of efficiency torque and cogging torque has been generated.

Keywords: Permanent Magnate Brushless DC Motor; Finite Element Analysis; Efficiency.

INTRODUCTION

BLDC motors are derived directly from the classical DC machines by replacing the commutators and brushes with an electronic power supply. The motor is often designed to have a trapezoidal back EMF waveform and the current waveforms are rectangular, with alternating polarity. The current polarity is switched in synchronism with the rotor position, by means of power semiconductors which are also used to regulate the current. Fig. 1 shows a typical example of PM BLDC motor. Permanent magnets (mounted on the rotor surface) are generally used for excitation.

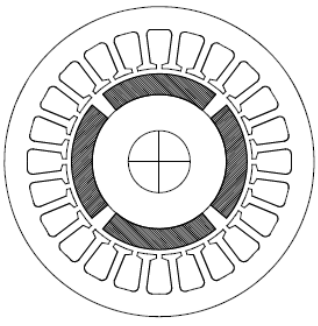

Figure 1: Brushless permanent-magnet motor

BASIC OPERATION OF THE BRUSHLESS DC MOTOR

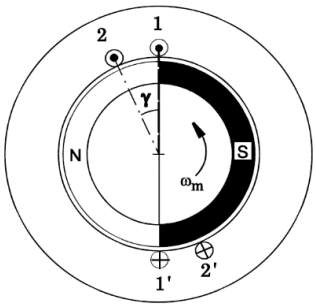

Figure 2:Back EMF generation in PMBLDC motor

Fig. 2 shows a 2-pole motor with a magnet rotating counter-clockwise at the instant when the flux-linkage with coil 1 is at a negative maximum.

The magnet is shown with an arc $\beta_M = 180^o$ elec., and the coil-pitch is also 180^o elec, so that the flux-linkage R1 of each coil varies with a triangular waveform as the rotor rotates: By Faraday's Law the EMF induced in coil 1 is

$$e_1 = \frac{d\varphi_1}{dt} = \omega_m \frac{d\varphi_1}{d\theta}$$

where Tm is the angular velocity in mechanical rad/s and 2 is the rotor position in mechanical radians. If the flux-linkage is varying linearly with rotor position, the induced EMF is constant. When the flux-linkage reaches a maximum, it starts to decrease at the same absolute rate, and the EMF changes polarity. The result is a square wave generated EMF. The EMF can be calculated from the airgap flux distribution. If B_g is the average flux-density over one pole-pitch, the airgap flux Mg is given by

$$\emptyset_g = \int_0^{\frac{\pi}{p}} B(\theta) r d\theta L_{stk} = B_g \times \frac{\pi D L_{stk}}{2p}$$

where r is the stator bore radius and D (= 2r) is its diameter; L_{stk} is the stack length, and p the number of pole-pairs. The peak flux-linkage of coil 1 is R1 max = Tc Mg, and if the linear variation of R1 with 2 is

$$\varphi_1(\theta) = \frac{p\theta}{\frac{\pi}{2}}\varphi_{1max}$$

Then the peak coil EMF is

$$e_1 = \omega_m \times \frac{2p}{\pi} \times T_c \emptyset_g$$

For a machine with Tph turns in the series per phase, the peak EMF/phase can be written as

$$e_{1(pk)} = \omega_m \times \frac{2p}{\pi} \times T_{ph} \emptyset_g$$

$$e_{LL(pk)} = 2e_{1(pk)} = k_E \omega_m$$

Where k_E is the back-EMF constant in Vs/rad:

$$k_E = \frac{4pT_{ph}\,\emptyset_g}{\pi}$$

The electromagnetic power is $e_{LL(pk)}$I and the electromagnetic torque is

$$T_e = \frac{e_{LL(pk)}I}{\omega_m} = k_T I$$

Where k_T=k_E is the torque constant in Nm/A. When driven this way with "two phases on", the motor behaves very much like a permanent- magnet DC commutator motor. The torque is produced in blocks 60° wide, and there are 6 such blocks every electrical cycle.

PROCESS OF TORQUE PRODUCTION

Eqn. of Te is an example of an ideal electromechanical device that converts instantaneous electric power into instantaneous mechanical power, without loss or storage. The same idea is used to develop a torque equation for sinewave brushless motors. In general, for a non-salient-pole brushless PM machine with *m* phases, the electromagnetic power is a result of the interaction between all the phase currents *i*1, *i*2 ,...*i*m and the corresponding EMF'S *e*1, *e*2,...*e*m generated by the rotation of the magnets. Thus

$$T_e\omega_m = e_1 i_1 + e_2 i_2 + e_3 i_3 + \cdots + e_m i_m$$

In the "square wave" operation described above, with "two phases on" at any time, we have a 60^0 interval, so that

$$T_e\omega_m = e_1 I - e_2 I = (e_1 - e_2)I = e_{LL} I,$$

where e_{LL} is the line-line EMF between phases 1 and 2. Te is, of course, the instantaneous torque and not the average torque. The average electromagnetic torque (averaged over one or more revolutions) is,

$$T_{avg} = \frac{1}{2\pi}\int_0^{2\pi} T_e\ (\theta) d\theta$$

SIMPLE MAGNETIC CIRCUIT ANALYSIS

The magnet flux can usually be calculated approximately by means of a simple magnetic circuit, such as the one in Fig.3. Under open-circuit conditions it is usually sufficient to consider only one pole, and to make use of symmetry. Thus in Fig.3 the quadrature or inter polar axes qq can be assigned zero magnetic potential. The method is to reduce the equivalent circuit as far as possible by means of series/parallel connections and conversions between Thévenin's and Norton's equivalents, and then to "work back up the chain" to extract the required branch fluxes. When the magnetic circuit is saturated the nonlinear reluctances can be calculated recursively, updating them by means of the BH curve together with the appropriate geometric dimensions. The method is fast and robust, and is a good starting point. Its main weakness is the use of lumped parameters for components in which the field may be far from uniform. Armature reaction is not easily incorporated, and although a separate inductance calculation can be used to model the circuit effects of armature reaction, this approach will overlook any modification of the flux distribution by the stator current. The magnetic equivalent circuit also does not recognize the spatial distribution of airgap flux.

It is shown later that this can be imposed independently by a semi-empirical shape function; but when this is done, it is important to be sure that the integral of this function and its peak values are consistent with the values predicted by the magnetic equivalent circuit.

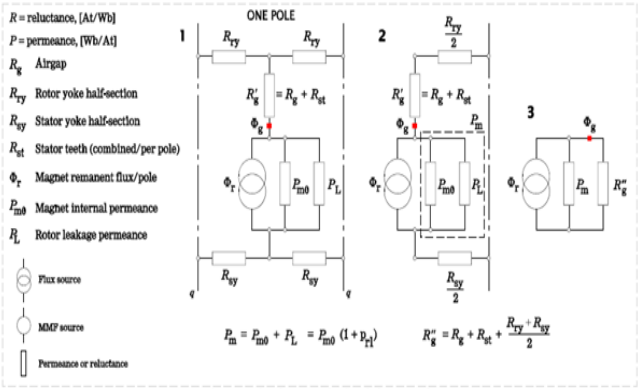

Figure 3: Magnetic equivalent circuit

From fig. 3 , the flux through the magnet is, in general,

$$\emptyset_m = \emptyset_g + \emptyset_L = \emptyset_g + \frac{P_L}{P_{m0} + P_L}(\emptyset_r - \emptyset_g)$$
$$= \emptyset_g + \frac{prl}{1 + prl}(\emptyset_r - \emptyset_g).$$

Where Pmo is the internal magnet permeance $\mu_0\ \mu_{rec}\ A_m/\ L_m$ and p_{rl} is the per unit leakage permeance

$$p_{rl} = \frac{P_L}{P_{mo}}$$

In the single case of a single external reluctance Rg, the air gap flux is

$$\emptyset_g = \frac{1/R_g}{1/R_g + P_{m0} + P_L}\emptyset_r = \frac{1/R_g}{1/R_g + P_m}\emptyset_r = \frac{1}{1 + P_m R_g}\emptyset_r$$
$$= \frac{1}{1 + (1 + p_{rl})P_m R_g}\emptyset_r$$

The leakage factor id defined in general as the ratio of airgap flux to magnet flux:

$$f_{LKG} = \emptyset_g/\emptyset_m$$

If Øg and Øm computed in terms of f_{LKG} then new expression will be

$$\emptyset_m = \frac{1}{1 + f_{LKG} P_{m0} R_g}\emptyset_r$$

And

$$\emptyset_g = \frac{f_{LKG}}{1 + f_{LKG} P_{m0} R_g}\emptyset_r$$

For surface-magnet motors it is usually more convenient to use eqns. above which characterize the leakage in terms of f_{LKG}, which typically has a value in the range 0.85 to 0.95. But for interior-magnet motors it is more convenient to use above eqns. which characterize the leakage in terms of p_{rl}, because p_{rl} can often be estimated from the geometry. In interior-magnet motors the leakage path represented by PL in Fig. 3 almost always includes a saturable element in the form of a magnetic bridge, as in Fig. 4, and one way to deal with this is to assume that the bridge is permanently saturated with a flux-density of, say, 1T, and to subtract the flux in the bridge (or bridges) from Mr, with which they are in parallel.

Finally, given that Mg = BgAg and Mr = BrAm, it gives another convenient formula for Bg:

$$B_g = \frac{f_{LKG}}{1 + f_{LKG} P_{m0} R_g} \times \frac{A_m}{A_g} B_r$$

NONLINEAR CALCULATION

The magnetic circuit in Fig. 4 is drawn for half of one Ampère's Law contour, representing the MMF drops associated with one airgap. The magnet is represented by a Thevenin equivalent circuit in which F_{ma} is the "open-circuit" MMF and $R_{m0} = 1/P_{m0}$. The flux densities in the yoke and teeth sections are calculated from their permeance areas, and the associated MMF drops F are obtained using the nonlinear BH curve of the steel. Bridge leakage in interior-magnet motors is modelled by the flux source Mb. The total magnetizing force in the magnet is calculated as

$$H_m = \frac{F_g + F_{SY} + F_{RY} + F_{ST}}{L_m}$$

The circuit is solved iteratively. The basic result of the nonlinear magnetic circuit calculation is the airgap flux Mg and from this the average flux density over the magnet pole arc can be calculated.

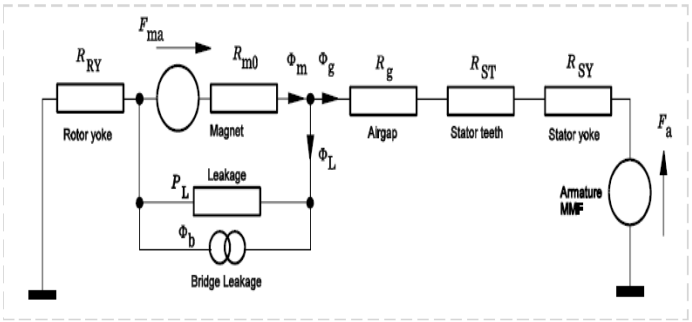

Figure 4: Non-linear equivalent circuit

AIRGAP FLUX DISTRIBUTION USED WITH SIMPLE MAGNETIC EQUIVALENT CIRCUIT

It has already been pointed out that the magnetic equivalent-circuit method does not recognize the spatial distribution of flux. To maintain the simplicity and speed of the method, it is possible to impose a distribution function of arbitrary shape, which can subsequently be modified or corrected by comparison with test or finite-element data. Such a distribution function is shown in Fig. 5 in which *b* is the normalized value of the flux-density

$$b = \frac{1}{2}\left[1 - e^{-\frac{\theta - \theta_a}{a}}\right], \theta_a < \theta < \frac{\pi}{2}\ ;$$

$$b = \frac{1}{2}\left[1 - e^{-\frac{\theta - \theta_a}{a}}\right], 0 < \theta < \theta a\ .$$

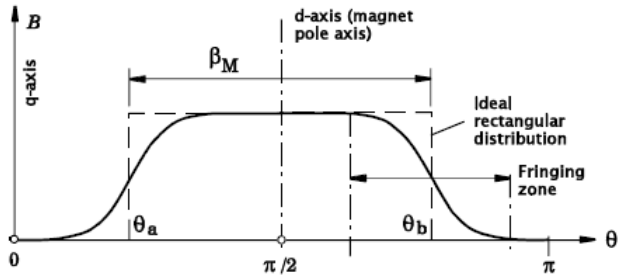

Figure 5: Airgap flux distribution

EQUIVALENT AMPERE-CONDUCTOR DISTRIBUTIONS

The magnet can be replaced by a current sheet K = M × n [A/m], where ***M*** is the magnetization vector inside the magnet and ***n*** is the unit vector normal to the magnet surface. Since ***M*** and ***n*** are both always in the *x, y* plane, transverse to the axis of rotation, ***K*** is always in the *z* direction along the axis of rotation, i.e. ***K*** = (0,0, *K*). ***M*** is the actual magnetization of the magnet, which includes an induced component due to the demagnetizing field of the external magnetic circuit. Unfortunately, this is not known a priori. However, if the recoil permeability is near 1, the susceptibility Pm of the magnet is nearly zero, and the induced magnetization is small. On open-circuit the magnets are normally worked between *B*r/2 and *B*r, and he uses the average magnetization over this range, i.e., *M* = *k*m*M*0 = *k*m *B*r/μ 0 where *k*m = (1 + 0.75 Pm)/(1 + Pm). Note that *M* is equivalent to the "apparent coercivity" H_{ca}, i.e. the coercivity that the magnet would have if its recoil line was straight throughout the second quadrant with relative permeability μ_r. The value of the susceptibility Pm and the constant *k*m can be seen in Table 1 for typical values of μ_r. For most magnets μ_r does not exceed 1.1, so the maximum error from this approximation is less than 2.5%.

Table 1: Magnetic field constant

μr	**χm**	**Km**
1	0	1
1.05	0.05	0.988
1.1	0.1	0.977
1.2	0.2	0.958

TORQUE AND EFFICIENCY

The torque is depending on the size of machine and the basic equation of the torque is as follows:

$T = kD^2L$

Where D is the diameter of machine and L is the length of machine and k is constant.

Now due to the different parameter the torque developed in the machines

$T= N_m k_d k_p k_s B_g LR_{ro} N_{spp} n_s i$

Ohmic loss

$P_r = N_{ph} I_{ph}^2 R_{ph}$

Where R_{ph} is phase resistance, I_{ph} is phase current, N_{ph} is number of phase.

Core loss is

$$P_{cl} = \rho_{bi} V_{st} \Gamma(B_{max}, f_e)$$

Where ρ_{bi} is mass density of stator material (kg/m3), Vst is stator volume, $\Gamma(B_{max}, f_e)$= core loss density (watt/kg) of stator material at B_{max} and frequency f_e Efficiency at rated torque and rated speed is

$$\eta = \frac{T\omega_m}{T\omega_m + P_r + P_{cl} + P_s}.100\%$$

Where Ps is the stray loss, composed of wind age, friction, and other less dominant loss components.

SIMULATION WITH MATLAB

1.1 kW, 3000 RPM, 3phase, 2 pole Permanent Magnet Brushless DC motor is taken study purpose. The stator and rotor outer radius is 95mm and 60mm respectively. From the equation of the machine parameter, the efficiency and the torque has been calculated. After that the usages of FEM tool the efficiency and the torque is to be calculated.

Table 2: Output of the analytical method

Parameter value	**Parameter value**
Stator inner radius(mm)	60.5
Tooth width at surface(mm)	11
Width of stator back iron (mm)	22
Tooth width at bottom(mm)	7.4
Rotor inner radius(mm)	31
Slot width at bottom(mm)(Wsb)	21
ds= conductor slot depth(mm)	47
Ohmic loss (Watt)	118.75
Core loss(Watt)	59.86
T= torque(Nm)	**8.5014**
efficiency	**83.762%**

The efficiency and the torque are calculated, and cogging torque waveform is as shown in fig 6, 7, 8 respectively.

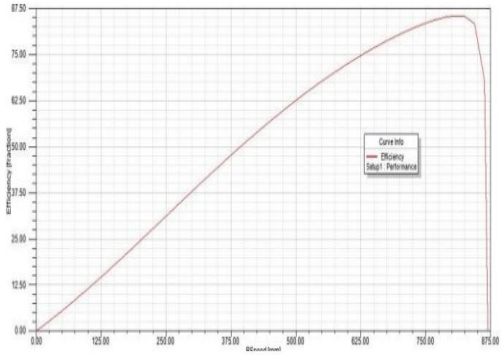

Figure 6: PM Brushless motor efficieny

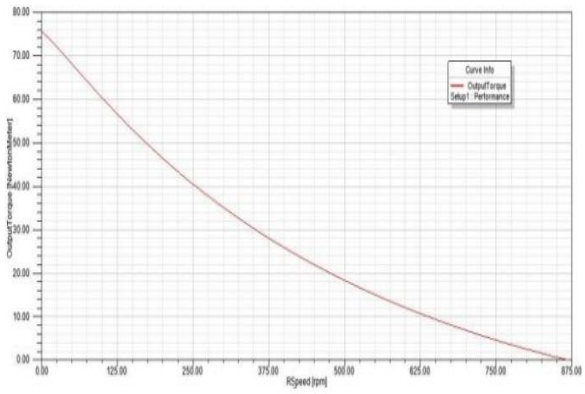

Figure 7: PM Brushless motor Torque

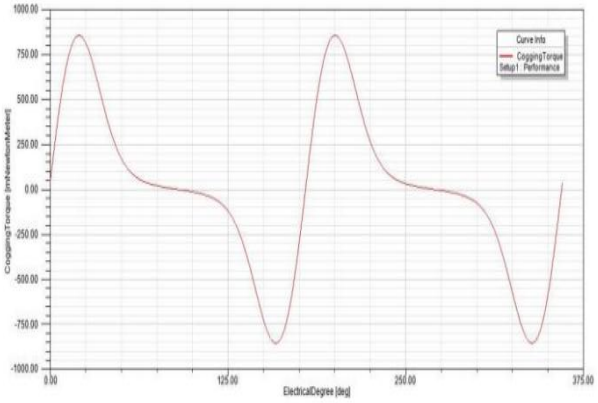

Figure 8: Cogging torque of PM Brushless motor

FINITE-ELEMENT ANALYSIS USING SPEED

In the analytical method, it is not well adapted to deal with saturation effects, but the method is nevertheless still useful, either for machines where saturation is not important, or where simplified allowances can be made for it. The simple magnetic circuit model can make crude allowances for saturation, but for thorough analysis of the magnetic field the finite element method is by far the most powerful. It is particularly effective in computing the details of local geometric features and the effects of arbitrary distributions of ampere-conductors and magnetization patterns. These details continually increase in importance, partly because of competitive pressure to improve performance and cost-effectiveness, but also because of the need to reduce torque ripple and acoustic noise.

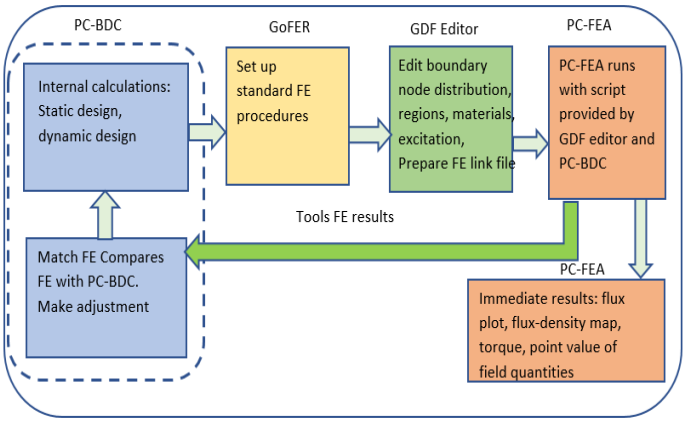

Figure 9*:* Finite element process with SPEED

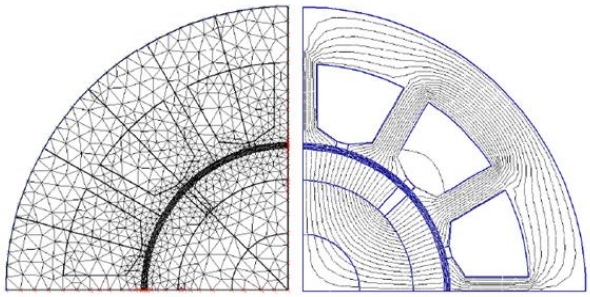

Figure 10: Finite-element mesh for PMBLDC motor and Magnetic field (open circuit)-SPEED

Fig. 10 shows typical examples of finite-element computations for a simple brushless permanent-magnet motor on open-circuit, and Fig. 11 shows the comparison of the airgap flux-density distribution obtained by the finite-element and magnetic-circuit methods. The finite-element solution includes the effect of the slot-openings, which is absent from the analytical solution.

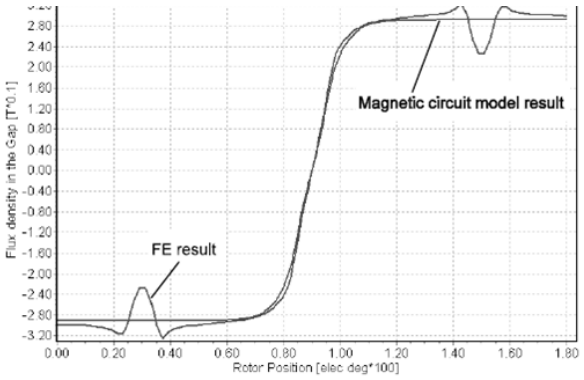

\

Figure 11: Comparison of finite-element and magnetic-circuit model

WINDINGS

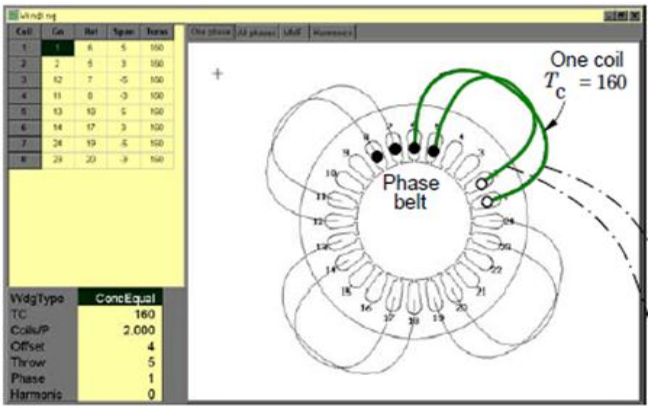

Figure 12: Motor stator winding schematic

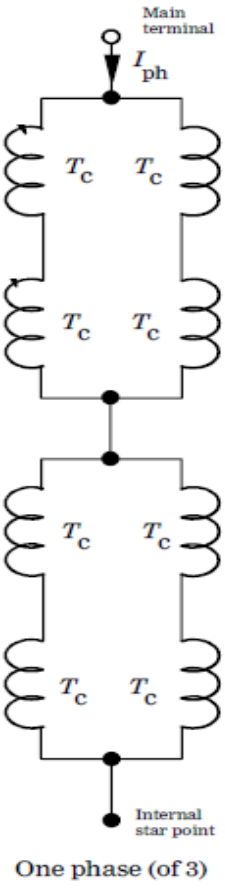

Figure 13: Stator equivalent circuit (one phase)

Turns / Coil = T_c , Coils / Pole = 2, Parallel paths a = 2, Coils / Phase = 8

Turns in series / phase $T_{ph} = \frac{T_c \times Coils/pole \times No.of\ poles}{Parallel\ paths}$ = (160X2X4)/2 = 640.

One turn = 2 conductors ("go" and "return")

Each turn (and each conductor) carries the current I_{ph} / a.

Total number of conductors Z= T_{ph} X 2 X N_{ph} X a = 640 X 2 X 3 X 2 = 7680.

The subject of windings forms a convenient bridge between the square wave drive and the sinewave drive, because the layout of the stator winding has a strong influence on the all-important EMF waveform. Fig. 9 shows some of the terms used relating to motor windings. Classical windings for AC motors were of the so-called distributed type, usually with several slots/poles and several conductors per phase belt, either lap-wound or concentric, as in Fig. 10. This type of winding was developed for classical synchronous machines and induction machines, with the aim of minimizing EMF harmonics and MMF harmonics. Square wave brushless PM motors require a flat-topped or trapezoidal EMF waveform, which can be obtained with a winding such as that in Fig. 9, which essentially has a small number of conductors per phase belt spanning almost a whole magnet pole and several slots. This type of winding used to be termed concentrated, but the term concentrated has recently come to refer to coils wound around a single tooth, which is a very different type of winding. Because the number of slots/pole/phase is often quite small, and because of the widespread use of single-tooth windings with fractional slots/pole for both square wave and sinewave motors, the practical differences between these windings are often not apparent.

The winding shown in Fig. 9 has three phases, of which only one is shown. There are four poles (corresponding to the number of magnet poles), and for each pole there is a group of 2 coils which are said to be "concentric" because of the way in which the outer coil embraces the inner one. The outer coil in each pole-group in Fig. 10 has a span of 5 slots, and the inner one a span of 3 slots. Taking two coil groups together, and recognizing that adjacent coil-groups alternate in polarity, in Fig. 10 there are four coil-sides in adjacent slots all carrying current in the same direction, and these coil sides constitute what is known as a *phase-belt*. In this winding the phase belt is spread across 4 slot pitches, and since there are 24 slots covering 4 poles, this is 4/6 or 2/3 of a pole-pitch or 120 electrical degrees. In a perfectly concentrated winding (in the old sense of "concentric") the phase-belt would have a spread of zero: in other words, all the coil sides in that phase-belt would be in the same slot. Thus, the winding in Fig. 10 is a distributed winding.

To make a perfectly concentrated winding, again in the old sense of "concentric", the coils in Fig. 10 would all have to have a span of 6 slot-pitches: that is, they would be "full-pitch" coils. Only 4 slots would be occupied by any phase, and half the slots in the machine would be empty. As it is, every slot holds two coil-sides, one from each of two different phases (this is called a "double-layer" winding). The distribution of coil-sides is critical in the determination of the EMF waveform, and has a significant influence on the winding inductance and the mutual

inductance between phases. A full pitch concentrated winding produces an EMF time-waveform on open-circuit that is a replica of the spatial distribution of magnet flux-density around the airgap. It is possible to construct the EMF waveform of any symmetrical winding by adding together the EMF waveforms of an equivalent distribution of full-pitch coils.

RESULTS

Comparison of the output of the FEM and Analytical solution gives the exact idea about the FEM technique that how accurate it is.

Table 3: Comparison of two method

Speed	Efficiency	
	Mathematical	FEM
2400	78.61	80.16
3000	83.762	85.37
3400	86.64	89.31

CONCLUSION

The FEA of the BLDC motor was carried out to validate the design. The analysis covered mathematical modeling of equivalent circuit include the non-linear magnetic properties of the material. The analysis also included study of armature reaction effects on the magnetic design and thermal effects of the motor. The parameters obtained from the Mathematical model and Finite Element Analysis meets most of the required specifications. The study proves the usefulness of the proposed machines design procedure. Permanent Magnet Brushless DC motor with 1.1 kW rating and 3000 rpm rated speed has been designed and the result of efficiency torque and cogging torque has been generated.

REFERENCES

[1] C.M. Ong, Dynamic simulation of electric machinery, Prentice-Hall PTR, Upper Saddle River, NJ, 1998

[2] M.Norhisam, A. Nazifah, I. Aris, H. Wakiwaka, Effect of Magnet Size on Torque Characteristic of Three Phase Permanent Magnet Brushless DC Motor IEEE Student Conference on Research and Development (SCOReD), 293 – 296, 2010.

[3] P.C. Krause, Oleg Wasynczuk, Scott D Sudhoff, 'Analysis of Electric Machinery and Drive Systems', Second edition, IEEE press.

[4] Popescu M, D.M Ionel, TJE Miller, S.J. Dellinger and M.I. McGilp Improved finite element computations of torque in brushless permanent magnet motors, IEE Proc-Electr. Power Appl., Vol. 152, No 2, March/April 2005, pp. 271-276.

[5] Ionel D M, Popescu M, McGilp MI, Miller TJE and Dellinger SJ Assessment of torque components in brushless permanent-magnet machines through numerical analysis of the electromagnetic field, IEEE Transactions on Industry Applications, Vol. 41, No. 5, September/October 2005, pp.1149-1158.

[6] SPEED Tutorial B14: Interior Permanent-Magnet Motor (IPM): Calculating torque and saturation using the i-psi GoFER.

[7] SPEED Tutorial B18: Magnet losses in PC-BDC/PC-FEA.